9. Abrahams, J. P. & Leslie, A. G. W. *Acta Crystallogr. D* **52,** 30–42 (1996).
10. Cheetham, J. C. *et al.* NMR structure of human erythropoietin and a comparison with its receptor bound conformation. *Nature Struct. Biol.* (in the press).
11. De Vos, A. M., Ultsch, M. & Kossiakoff, A. A. Human growth hormone and extracellular domain of its receptor: crystal structure of the complex. *Science* **255,** 306–312 (1992).
12. Sprang, S. R. & Bazan, J. F. Cytokine structural taxonomy and mechanisms of receptor engagement. *Curr. Opin. Struct. Biol.* **3,** 815–827 (1993).
13. Rozwarski, D. A. *et al.* Structural comparisons among the short-chain helical cytokines. *Structure* **2,** 159–173 (1994).
14. Yoshimura, A. *et al.* Mutations in the Trp-Ser-X-Trp-Ser motif of the erythropoietin receptor abolish processing, ligand binding, and activation of the receptor. *J. Biol. Chem.* **267,** 11619–11625 (1992).
15. Baumgartner, J. W., Wells, C. A., Chen, C. M. & Waters, M. J. The role of the WSXWS equivalent motif in growth-hormone receptor function. *J. Biol. Chem.* **269,** 29094–29101 (1994).
16. Barbone, F. P. *et al.* Mutagenesis studies of the human erythropoietin receptor. Establishment of structure–function relationships. *J. Biol. Chem.* **272,** 4985–4992 (1997).
17. Middleton, S. A. *et al.* Identification of a critical ligand-binding determinant of the human erythropoietin receptor—evidence for common ligand-binding motifs in the cytokine receptor family. *J. Biol. Chem.* **271,** 14045–14054 (1996).
18. Grodberg, J., Davis, K. L. & Sykowski, A. J. Alanine scanning mutagenesis of human erythropoietin identifies four amino acids which are critical for biological activity. *Eur. J. Biochem.* **218,** 597–601 (1993).
19. Wen, D. Y., Boissel, J. P., Showers, M., Ruch, B. C. & Bunn, H. F. Erythropoietin structure–function relationships–identification of functionally important domains. *J. Biol. Chem.* **269,** 22839–22846 (1994).
20. Matthews, D. J., Topping, R. S., Cass, R. T. & Giebel, L. B. A sequential dimerization mechanism for erythropoietin receptor activation. *Proc. Natl Acad. Sci. USA* **93,** 9471–9476 (1996).
21. Elliott, S., Lorenzini, T., Chang, D., Barzilay, J. & Delorme, E. Mapping of the active site of recombinant human erythropoietin. *Blood* **89,** 493–502 (1997).
22. Clackson, T. & Wells, J. A. A hot spot of binding energy in a hormone-receptor interface. *Science* **267,** 383–386 (1995).
23. Watowich, S. S. *et al.* Homodimerization and constitutive activation of the erythropoietin receptor. *Proc. Natl Acad. Sci. USA* **89,** 2140–2144 (1992).
24. Narhi, L. O. *et al.* The effect of carbohydrate on the structure and stability of erythropoietin. *J. Biol. Chem.* **266,** 23022–23026 (1991).
25. Johnson, D. L. *et al.* Refolding, purification, and characterization of human erythropoietin binding protein produced in *Escherichia coli*. *Prot. Express. Purif.* **7,** 104–113 (1996).
26. Otwinowski, Z. & Minor, W. Processing of X-ray diffraction data collected in oscillation mode. *Methods Enzymol.* **276,** 307–326 (1997).
27. Collaborative Computational Project No. 4. The CCP4 suite: programs for protein crystallography. *Acta Crystallogr. D* **50,** 760–763 (1994).
28. Brunger, A. T. *X-PLOR, Version 3.1, A System for X-ray Crystallography and NMR* (Yale Univ. Press, New Haven, 1992).
29. Furey, W. & Swaminathan, S. Phases-95: a program package for processing and analyzing diffraction data from macromolecules. *Methods Enzymol.* **277,** 590–620 (1997).

Acknowledgements. We thank J. Philo, M. McGrath, P. Sprengeler, W. Welch, J. Rupert, L. Narhi, G. Rogers, M. Rohde, S. Jordan, K. Langley, R. Mackman and M. Venuti for valuable discussions. Structure analyses of Form 1 and Form 2 were independently performed at Axys Pharmaceuticals Inc. and Amgen Inc., respectively.

Correspondence and requests for materials should be addressed to R.S.S. (e-mail: rsyed@amgen.com) or R.M.S. (e-mail: stroud@msg.ucsf.edu). Coordinates have been deposited with the Brookhaven Protein Data Bank (accession numbers 1blw for Form 1 and 1eer for Form 2).

Tom40 forms the hydrophilic channel of the mitochondrial import pore for preproteins

Kerstin Hill*, Kirstin Model†, Michael T. Ryan†, Klaus Dietmeier†, Falk Martin†‡, Richard Wagner* & Nikolaus Pfanner†

* *Biophysik, Universität Osnabrück, FB Biologie/Chemie, D-49034 Osnabrück, Germany*
† *Institut für Biochemie und Molekularbiologie, Universität Freiburg, Hermann-Herder-Strasse 7, D-79104 Freiburg, Germany*
‡ *Fakultät für Biologie, Universität Freiburg, D-79104 Freiburg, Germany*

The mitochondrial outer membrane contains machinery for the import of preproteins encoded by nuclear genes[1–3]. Eight different Tom (translocase of outer membrane) proteins have been identified that function as receptors and/or are related to a hypothetical general import pore. Many mitochondrial membrane channel activities have been described[4–7], including one related to Tim23 of the inner-membrane protein-import system[5]; however, the pore-forming subunit(s) of the Tom machinery have not been identified until now. Here we describe the expression and functional reconstitution of Tom40, an integral membrane protein with mainly β-sheet structure. Tom40 forms a cation-selective high-conductance channel that specifically binds to and transports mitochondrial-targeting sequences added to the *cis* side of the membrane. We conclude that Tom40 is the pore-forming subunit of the mitochondrial general import pore and that it constitutes a hydrophilic, ~22 Å wide channel for the import of preproteins.

We expressed *Saccharomyces cerevisiae* Tom40 (ref. 8) in *Escherichia coli* cells (Fig. 1a, lane 2). Tom40, representing ~25% of total *E. coli* protein, accumulated in inclusion bodies and could be solubilized with urea. As Tom40 may be slightly similar to porins at the secondary structure level[9], we modified a method for the preparation and renaturation of *Rhodopseudomonas blastica* porin from *E. coli* inclusion bodies[10]. Tom40 was isolated to high purity (>95%) (Fig. 1a, lane 3). The two protein bands of minor abundance that are visible in the purified preparation of Tom40 (Fig. 1a, lane 3) are degradation products of Tom40. When diluted into the non-ionic detergent nonanoyl-*N*-methylglucamide (Mega-9), the recombinant Tom40 migrated as a single band on blue native electrophoresis and this band was indistinguishable from that of Tom40 that had been solubilized from mitochondria by Mega-9 (Fig. 1b). Circular dichroism analysis of Tom40 in urea and after dilution into Mega-9 indicated an efficient refolding of the protein upon dilution (Fig. 1c). We inserted Tom40 into liposomes by dilution of the urea-denatured protein into a mixture of Mega-9 and azolectin, with subsequent removal of the detergent. The circular dichroism spectrum of liposome-inserted Tom40 was comparable to that of Tom40 in Mega-9 (Fig. 1c). A secondary structure calculation according to ref. 11 indicated a predominance of β-sheet structure (>60%) and little α-helical structure (<5%) in the protein.

To assess whether Tom40 was properly reconstituted in the liposomes, we determined its topological orientation in liposomes in comparison to that of Tom40 in mitochondria. Treatment of mitochondria with trypsin cleaved a small peptide (relative molecular mass (M_r) ~2.5K) from Tom40 (Fig. 1d, upper panel, lanes 2, 3). The same cleavage occurred after recombinant Tom40 inserted into liposomes was treated with trypsin (Fig. 1d, lower panel, lanes 2, 3). The remaining fragment of Tom40 was protected by the membranes, as, after lysis of mitochondria or liposomes with Triton X-100, it was digested by trypsin (Fig. 1d, lane 4). Antibodies directed against the amino-terminal or carboxy-terminal regions (12 terminal amino-acid residues in each region) of Tom40 showed that the C-terminal epitope of mitochondrial Tom40 was retained in the fragment (Fig. 1d, upper panel, lanes 6, 7), whereas the N-terminal epitope was removed by trypsin (Fig. 1d, upper panel, lane 10). The same topology of Tom40 was seen in the proteoliposomes (Fig. 1d, lower panel, lanes 6, 7, 10). A quantitative assessment of the fragmentation of Tom40 in mitochondria and liposomes (including a consideration of the higher resistance of mitochondrial membranes to trypsin) indicates that at least 50–60% of the recombinant Tom40 was inserted into liposomes with the correct orientation (another fraction of recombinant Tom40 was fully digested by trypsin even in the presence of intact liposome membranes, probably representing Tom40 associated with the liposome preparation but not inserted into the membrane). Indeed, a preprotein specifically affected the channel activity only when added to the *cis* side of the membrane (that is, to the N terminus of Tom40) (see below). We conclude that the recombinant Tom40 molecules that were functionally incorporated into liposomes were asymmetrically inserted with the same relative orientation as in the outer mitochondrial membrane.

To determine whether reconstituted Tom40 could form a channel, we performed electrophysiological studies. After fusion of Tom40-containing liposomes with a planar bilayer, single-channel currents could indeed be measured (Fig. 2a). At membrane potentials below 100 mV, the channels were mainly open and we observed brief, flickering closures of the channel. When examined at higher time resolution (10 kHz), the current recordings showed subconductance levels (lower trace, Fig. 2a). The current traces show that

direct transitions between the two main conductance levels occur, indicating that these levels are (sub)conductant states of the same channel. At more negative membrane potentials, more subconductance levels were found (details not shown). With 250 mM KCl buffer on both sides of the membrane, the fully open channel showed a linear current–voltage relationship with slope conductance of $\Lambda = 360 \pm 3$ pS, whereas a value of $\Lambda = 150 \pm 2$ pS was observed for the most frequent subconductance level (Fig. 2b). In asymmetric buffers (250/20 mM KCl) the reversal potential was $E_{rev} = +40 \pm 1.3$ mV for the open single channel ($n > 60$; details not shown). Accordingly, the channel showed a selectivity for cations over anions ($P_{K^+} : P_{Cl^-} \approx 8 : 1$). The relative permeabilities for different cations calculated from the corresponding reversal potentials (Cs^+, 1.1: K^+, 1.0: Na^+, 0.7: Li^+, 0.5: tetraethylammonium (TEA^+), 0.25: tetrabutylammonium (TBA^+), 0.12) roughly reflect the relative mobility of these ions in water. Therefore these ions are likely to cross through the sufficiently wide channel without interaction with it.

Figure 2c shows the voltage dependence of the channel open probability. At a membrane potential of 0 mV, the channel was completely open, whereas it closed symmetrically at positive or negative membrane potentials. When the concentrations of permeant ions on both sides were raised, the channel conductance increased asymptotically to a saturation value of $\Lambda \cong 3.58 \pm 0.35$ nS (Fig. 2d). Using the model that the Tom40 channel is a uniform cylinder filled with a solution of bulk medium resistivity, its diameter can be calculated according to refs 12, 13; when using $\Lambda = 360$ pS (symmetrical 250 mM KCl; assumed length of 50 Å), a diameter of 12 Å is obtained. However, on the basis of calculations in ref. 14, which assume that the resistivity in the channel is five times the bulk resistivity, a pore diameter of 26 Å is obtained. An experimental assessment of the pore diameter using cations of various size showed that the Tom40 channels were permeable to TEA^+, TBA^+ and different polyamines (cadaverine, spermine), whereas the polycation poly(L-Lysin)$_{1000}$ partially blocked the channel. Using the polymer-exclusion method[15], we obtained a pore diameter of 22 ± 1.4 Å.

When we incubated Tom40 with antibodies against the N-terminal epitope of Tom40, the proteoliposomes were precipitated and no further bilayer fusions were seen. The calculated number of Tom40 molecules in the liposomes correlated well with the number of active channels observed after fusion of the proteoliposomes to the planar bilayer. Together with the high purity of the Tom40 preparation, these data exclude the possibility that a contaminating protein was responsible for the channel activity. Moreover, a polyhistidine-tagged version of Tom40, purified by an independent procedure, yielded channel activities that were indistinguishable from those obtained with authentic Tom40. The basic properties of the reconstituted Tom40 channel (selectivity, conductance and open probability) were highly reproducible in more than 500 different experiments. We conclude that Tom40 forms a cation-selective high-conductance channel with multiple conductance states.

We isolated outer membrane vesicles[16,17] and fused them to liposomes and then to a planar bilayer. We identified a channel (Fig. 2e, f) with the same conductance ($\Lambda = 224 \pm 10$ pS slope conductance, 250/20 mM KCl), cation selectivity ($E_{rev} = +40$ mV, 250/20 mM KCl, $P_{K^+} : P_{Cl^-} = 8 : 1$), and voltage dependence as the channel formed by purified Tom40. The open probability of the outer-membrane-integrated channel was about three- to fourfold

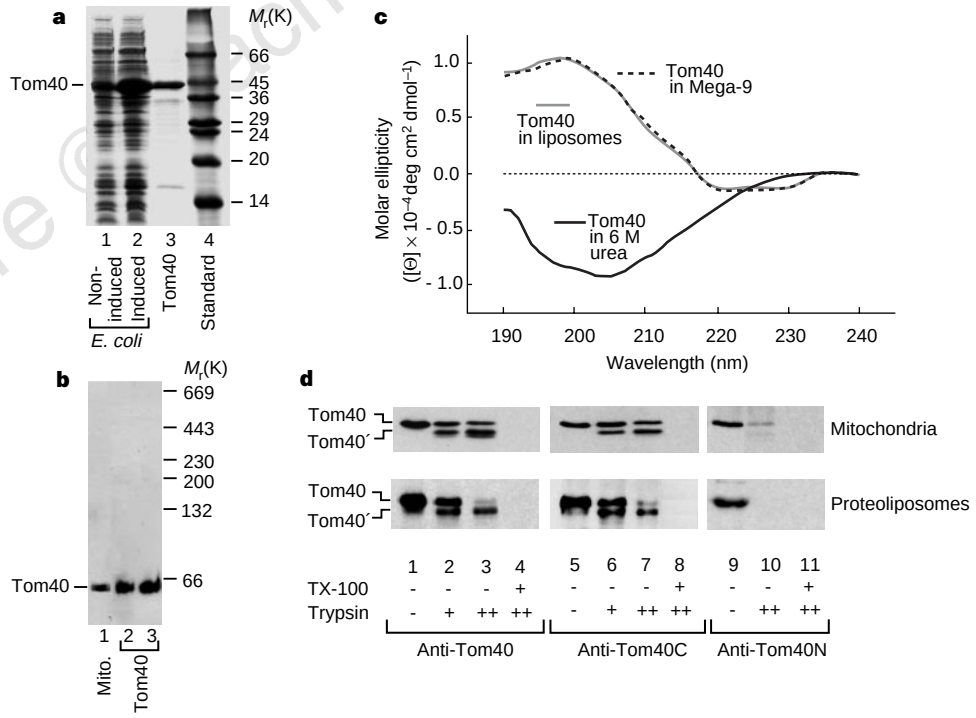

Figure 1 Expression of yeast Tom40 and its reconstitution into liposomes. **a**, Tom40 was analysed by Coomassie brilliant blue R250-stained SDS–PAGE. Lane 1, lysate from non-induced *E. coli* cells; lane 2, lysate from induced *E. coli* cells; lane 3, purified Tom40; lane 4, molecular size markers. **b**, Analysis of Tom40 in Mega-9 (1 μg in lane 2; 2 μg in lane 3) and in Mega-9-lysed mitochondria (200 μg in lane 1) by blue native gel electrophoresis and subsequent immunodecoration with antibodies against Tom40. **c**, Circular dichroism spectra of Tom40 in 6 M urea or 60 mM Mega-9 or reconstituted into liposomes. **d**, Orientation of Tom40 in mitochondria and liposomes. Treatment with trypsin was done as described in Methods (as controls, mitochondria or liposomes were lysed with Triton X-100 (TX-100) before the protease treatment). Immunodecoration was done with antibodies generated against whole Tom40 (left panel), the C-terminal epitope (middle panel) and the N-terminal epitope (right panel). The trypsin-generated fragment of Tom40 is termed Tom40′. The treatment with trypsin reduces the affinity of anti-Tom40N to Tom40 (compare lane 10 with lanes 3, 7), probably because of removal of a small number of N-terminal amino acids (not changing the apparent gel mobility).

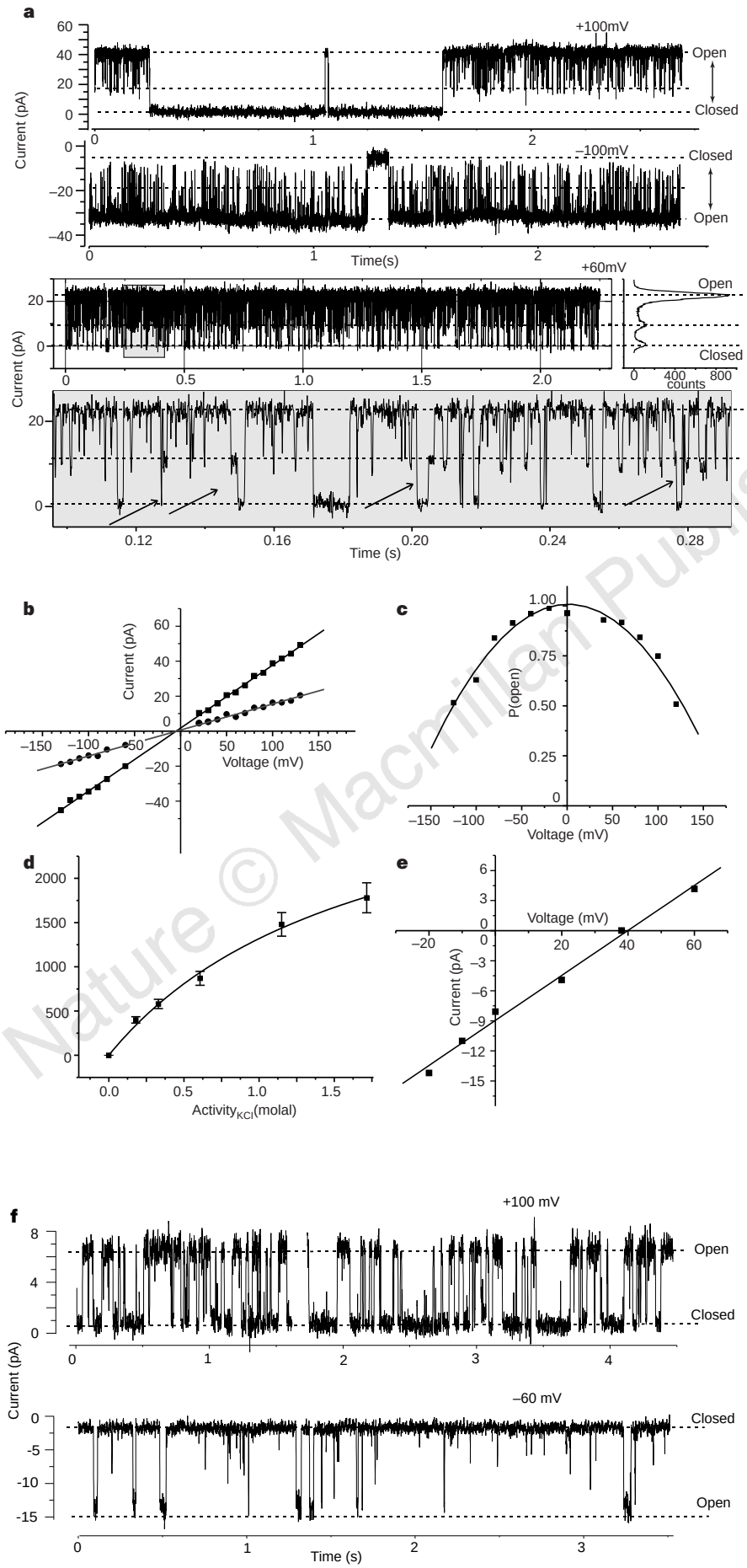

Figure 2 Tom40 forms a high-conductance cation-selective channel. **a**, Current traces from a bilayer containing one active Tom40 channel at different membrane potentials with 250 mM KCl, 10 mM $CaCl_2$ and 10 mM MOPS/Tris (pH 7.2) on both sides of the membrane. Applied membrane potentials are indicated. The lowest trace shows a timescale-expanded current recording from the trace above with high time resolution (10 kHz). Direct transitions between the different subconductance levels are marked with arrows. **b**, Current–voltage relationship of the fully open single channel (squares) and the most frequent subconductance level (circles) with 250 mM KCl on both sides of the membrane (averages of six independent bilayers, with standard errors of the means <4%). **c**, Voltage dependence of the probability for the Tom40 channel being in any of its open states. To approach equilibrium of channel gating with respect to the applied membrane potential voltages were applied for 5 min but only the current recordings of the last min were used to calculate P_{open} from the amplitude histograms (averages of at least three independent bilayers, with standard errors of the means <8% of the values). **d**, Saturation of the Tom40 conductance with symmetrically increasing KCl activities on both sides of the membrane. Bath solutions were changed by perfusion (three times the volume of the chamber). Data are averages of slope conductances from four different bilayers. **e**, **f**, Isolated outer mitochondrial membranes[16,17] were fused with preformed liposomes by freeze-thawing and subsequently sonicated in a water bath. Such liposomes were fused with the bilayer and current recordings were performed in 250 mM KCl, 10 mM $CaCl_2$/20 mM KCl (*cis*/*trans* chamber) and 10 mM MOPS/Tris (pH 7.2). **e**, Current–voltage relationship of the outer mitochondrial membrane cation-selective channel (data points are averages of at least four independent bilayers, with standard errors of the means <3–5% of the values). **f**, Single-channel current recordings from a bilayer containing a single copy of the outer mitochondrial membrane cation-selective channel.

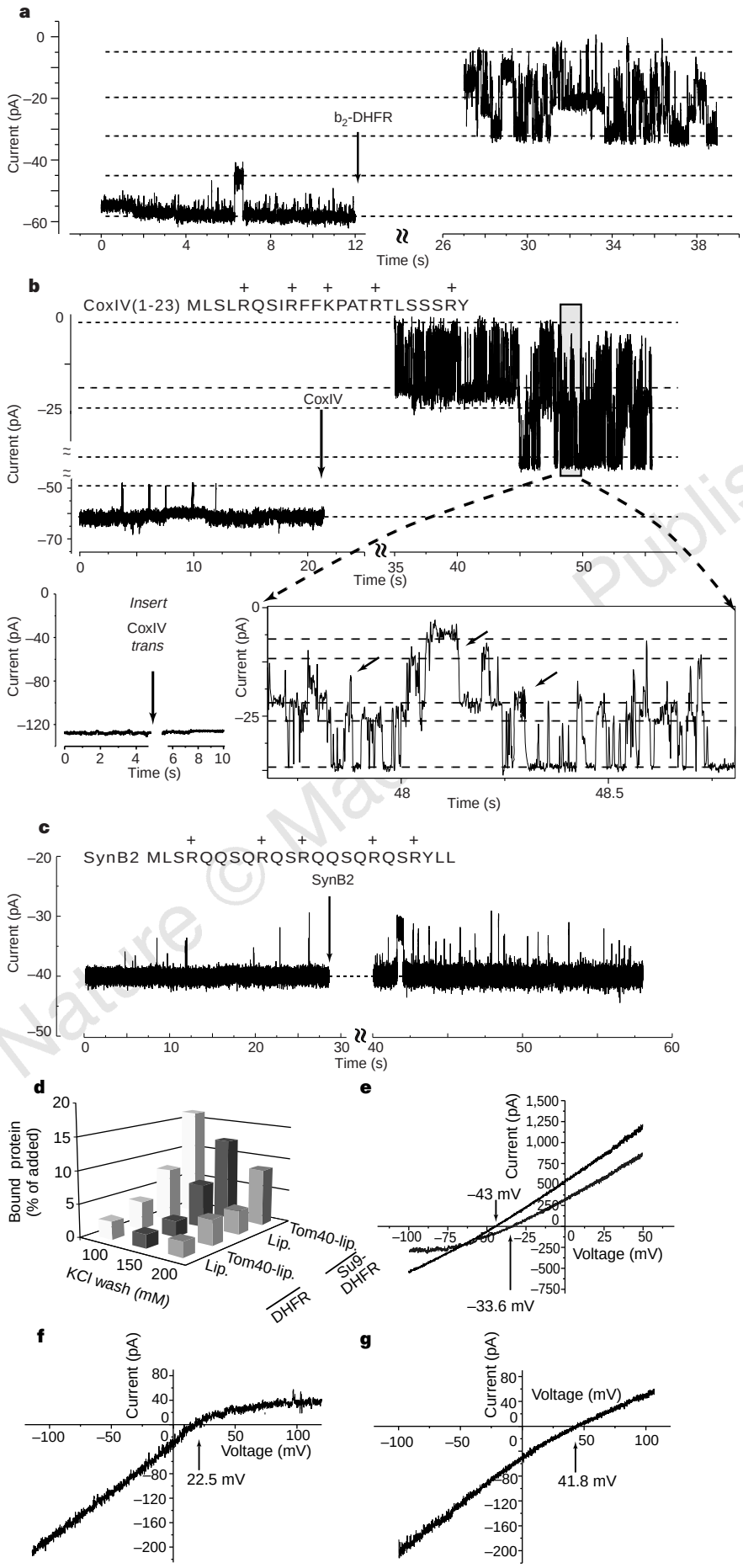

Figure 3 The Tom40 channel is sensitive to and transports a presequence peptide. **a–c**, Current traces from bilayers containing active Tom40 channels before and after addition of preprotein/peptides (b_2-DHFR, CoxIV, SynB2) bathed in 250 mM KCl, 10 mM $CaCl_2$/20 mM KCl (*cis*/*trans* chamber) and 10 mM MOPS/Tris (pH 7.2); holding potential $V_h = 0$ mV. After addition of the preprotein/peptides, the bath solution was vigorously stirred for 10 s. Dotted horizontal lines indicate the levels of the main conductances. **a**, Addition of 15 μM b_2-DHFR to the *cis* compartment; average current reduction 52%. **b**, Addition of 15 μM CoxIV(1–23) to the *cis* compartment; average current reduction 51% ($n = 10$, s.e.m. 3%). Inset, addition of CoxIV(1–23) to the *trans* compartment (no current reduction). **c**, Addition of 15 μM SynB2 (no current reduction). The amino acid sequences of CoxIV(1–23) and SynB2 are shown in the single-letter code, with positive residues indicated. **d**, ^{35}S-labelled Su9–DHFR and DHFR were incubated with liposomes (lip.) containing reconstituted Tom40 or with an equal amount of liposomes lacking Tom40. After washing of the liposomes with KCl as indicated, the amount of bound Su9–DHFR and DHFR was quantified by digital autoradiography. The total amount of Su9–DHFR or DHFR added was set to 100%. After subtraction of protein bound to Tom40-free liposomes, 6.6% of Su9–DHFR and 1.1% of DHFR bound to Tom40-containing liposomes (on average). **e–g**, Translocation of CoxIV(1–23). Here voltages refer to the *cis* compartment. Voltage ramps ($\Delta V = 1$ mV s^{-1}) were applied across bilayers containing multiple copies of the active Tom40 channel. **e**, Recording from a bilayer containing about 60 active copies of the Tom40 channel in asymmetrical 250 mM/20 mM KCl, 10 mM MOPS/Tris (pH 7.2) (*cis*/*trans*); upper trace, control; lower trace, addition of 50 μM CoxIV to the *trans* compartment. **f**, **g**, Recording from a bilayer containing about eight active copies of the Tom40 channel in asymmetrical 20 mM/250 mM KCl, 10 mM MOPS/Tris (pH 7.2) (*cis*/*trans*). **f**, Addition of 10 μM CoxIV(1–23) to the *cis* compartment. **g**, Control.

lower than that of purified Tom40, indicating that the presence of other Tom proteins may exert a regulatory effect on the gating of the channel.

We determined whether the channel formed by reconstituted Tom40 responded to the presence of a mitochondrial preprotein. We added a fusion protein containing part of the precursor of cytochrome b_2 together with dihydrofolate reductase (b_2–DHFR)[18] to the planar bilayer. This fusion protein strongly reduced the channel open probability and concomitantly increased the frequency of channel gating (Fig. 3a). This markedly reduced the total current passing through the Tom40 channel. This effect was only seen when the preprotein was added to the *cis* side of the planar bilayer (N terminus of Tom40). The effect was reversed when the preprotein was removed by perfusion of the chamber bath solution.

To determine the specificity of this inhibition by a preprotein, we compared the effects of two synthetic peptides on the channel activity, namely, a peptide corresponding to the mitochondrial-targeting signal of cytochrome oxidase subunit IV (CoxIV(1–23)) (Fig. 3b), and a related peptide (SynB2) with the same number of positively charged residues (Fig. 3c) that was, however, unable to direct the import of mitochondrial preproteins[19,20]. CoxIV(1–23) efficiently reduced the channel open probability and increased the frequency of channel gating in the same way as did b_2–DHFR (Fig. 3b), whereas SynB2 did not (Fig. 3c). The inhibitory effect of CoxIV(1–23) was, again, only seen when the peptide was added to the *cis* compartment (Fig. 3b). By adding b_2-DHFR or CoxIV(1–23), we reduced currents in both directions, whereas currents were not reduced on addition of 15 μM SynB2. The reduction in the mean currents was nonlinearly dose-dependent and 15 μM b_2–DHFR and CoxIV(1–23) led to roughly half-maximal inhibition. A large conductance channel, PSC, with some preference for cations has been localized to the outer membrane and shown to be blocked by the presequence peptide CoxIV and the non-mitochondrial basic peptide dynorphin B (ref. 6). The Tom40 channel, however, was not affected by dynorphin B (at 15 μM; $n = 5$), supporting the conclusion that Tom40 interacts specifically with presequences, but not with other basic peptides.

Crosslinking studies in intact mitochondria showed that there is a specific interaction between Tom40 and mitochondrial presequences[21]. To test biochemically whether reconstituted Tom40 interacts with a mitochondrial preprotein, we incubated a fusion protein, consisting of the presequence of F_O-ATPase subunit 9 (Su9) and the non-mitochondrial passenger protein dihydrofolate reductase (DHFR), with Tom40-containing liposomes or Tom40-free liposomes. A large excess of bovine serum albumin was included in the binding assay to exclude the possibility that unspecific protein–protein interactions were measured. After washing the liposomes with KCl to reduce the association of Su9–DHFR with the phospholipid headgroups, we observed a significant association of Su9–DHFR with the Tom40-containing liposomes (Fig. 3d; 200 mM KCl). The binding was mediated by the presequence, as DHFR alone showed only background levels of binding (Fig. 3d).

The complete translocation of presequence-containing preproteins across the outer mitochondrial membrane requires the import-driving system of the inner membrane (Tim–Hsp70 (heat-shock protein 70) machinery). When using isolated outer membrane vesicles, only translocation of the presequence could be monitored[22]. We therefore determined whether the purified Tom40 could also translocate presequences. We measured the current–voltage relationship of Tom40-containing bilayers in the presence of 5–100 μM CoxIV(1–23) or 5–100 μM SynB2 on either side of the membrane. When 10 μM CoxIV(1–23) was added to the *cis* compartment containing 20 mM KCl (250 mM KCl *trans*), a pronounced change in the reversal potential was observed ($\Delta E = 18 \pm 2$ mV; $n = 11$) (Fig. 3f, g), and at positive potentials, which force the fivefold positively charged polypeptide towards the *trans* compartment, a drastic decrease in the current was observed (Fig. 3f, g). When the experiments were done in the opposite direction, a significantly smaller change in the reversal potential occurred (Fig. 3e) ($\Delta E = 9 \pm 2.5$ mV; $n = 9$) and, concomitantly, the reduction in current was less pronounced (Fig. 3e).

These results show that CoxIV(1–23) can interact with the channel pore from both sides; however, its affinity for the pore is about one order of magnitude higher when it is on the *cis* side of the pore indicating that the presequence may interact with negatively charged groups of the pore. As <10 μM of CoxIV(1–23) on the *cis* side (low salt) changed the reversal potential markedly, it is unlikely that this effect is due only to the permeation of the peptide. As CoxIV(1–23) did not completely block the channel pore, we estimate, from comparison with the current–voltage relationship of spermine, that the presequence peptide can permeate the channel at significant rates (up to 10^3–10^4 molecules per s at a driving force of 100 mV). After addition of SynB2 (50 μM) to either compartment ($n = 5$ each side), $\Delta E = 10 \pm 3$ mV. Thus, only CoxIV(1–23) shows high affinity for the pore (*cis* side). Moreover, the suppression of the current by SynB2 was about 10–50-fold more pronounced than that by CoxIV(1–23), indicating that SynB2 is transported at a considerably slower rate than the presequence peptide. The studies using low membrane potential (Fig. 3b) show that the presequence peptide selectively binds to Tom40 from the *cis* side and thereby alters the gating of the channel, whereas it is rapidly translocated through the channel when driven by higher voltage (Fig. 3f).

Tom40 is, to our knowledge, the first membrane protein of the mitochondrial protein import machinery that has been purified and reconstituted in a functional form. It forms a hydrophilic cation-selective channel. The size of the channel diameter (~22 Å) indicates that typical folded proteins cannot permeate; precursor polypeptides may pass through in an α-helical conformation or in an extended conformation. A piece of double-stranded DNA (diameter ~20 Å) covalently linked to a preprotein has been imported into mitochondria[23]. The size of the Tom40 channel seems to be sufficient to allow passage of the DNA. Recently, a Tom complex containing about seven different subunits was isolated from *Neurospora crassa* mitochondria. Negative stain electron microscopy showed stain-filled pits with an apparent diameter of ~20 Å that may represent import pores[24]. We propose that the pores were formed by Tom40. In the protein-import machinery of the chloroplast outer-envelope membrane, Toc75 (OEP75) was identified as the pore-forming subunit[13]. Toc75 has mainly β-sheet structure, like Tom40, but Toc75 and Tom40 share no sequence homology and activation of the Toc75 channel depends completely on a membrane potential. The calculated channel diameter for Toc75 is smaller (~10 Å) (ref. 13) than that of Tom40, whereas endoplasmic reticulum protein-transport channel, formed by the hetero-oligomeric Sec61p complex, has a calculated diameter of 20–60 Å (ref. 25).

Tom40 was identified as an outer-membrane protein that is near to a preprotein in transit[26]. The mature part[26] and the presequence[21] of a preprotein were crosslinked to Tom40, and Tom40 was shown to be an essential component of the multisubunit Tom machinery[8,17,27,28]. In addition, four other Tom proteins, Tom70, Tom22, Tom20 and Tom5, have been found to be crosslinked to preproteins[16,17,28,29]. Despite the complexity of the preprotein translocase of the mitochondrial outer membrane, it is now possible to assign individual functions to these Tom proteins: Tom70, Tom20 and Tom22 have receptor/binding functions, as shown using purified cytosolic and intermembrane space domains[20,30]; Tom5 is a mediator between receptors and the import pore[17]; and Tom40 forms the hydrophilic channel of the general import pore for preproteins. The affinity of Tom40 for mitochondrial-targeting sequences added to the *cis* side is close to the range of affinities seen with several Tom receptors[20]. We suggest that Tom40 is part of the proposed chain of multiple interaction sites for preprotein

transport across the outer membrane[17,29,30]. The asymmetric affinity of Tom40 for targeting sequences favours transmembrane transport in the *cis* to *trans* direction and renders Tom40 an important component that contributes to the directionality of mitochondrial-preprotein import. □

Methods

Expression and reconstitution of Tom40 in liposomes. A 1,164-base-pair genomic fragment, encompassing the open reading frame of *TOM40*, was amplified with *Pfu*-polymerase, subcloned into the vector pET11a and transformed into *E. coli* BL21(DE3). After induction with isopropyl-β-D(−)-thiogalactopyranoside, Tom40 was purified by a method adapted from ref. 10. Inclusion bodies were isolated, extensively washed in buffer containing Triton X-100 and solubilized in urea buffer (8 M urea, 50 mM Tris/HCl pH 8.0, 1 mM EDTA and 100 mM dithiothreitol (DTT)). The pH was gradually lowered to 6.5, followed by centrifugation at 50,000*g*, and the supernatant containing purified Tom40 was dialysed against 6 M urea, 50 mM Tris/HCl pH 8.0, 1 mM EDTA and 2 mM DTT. Tom40 in urea was diluted tenfold in Mega-9 buffer (80 mM Mega-9, 10 mM MOPS/Tris pH 7.0, 1 mM EDTA and 100 mM DTT) and analysed by blue native gel electrophoresis[18].

Purified Tom40 was resuspended in 80 mM Mega-9, 6 M urea and 10 mM MOPS/Tris pH 7.0 and reconstituted in liposomes by the dialysis technique. Briefly, small unilamellar liposomes were obtained from purified azolectin (Sigma, type IV S) as described[13] and were lysed in Mega-9. Tom40 was diluted ~50-fold into the mixture and proteoliposomes were then formed by dialysis. The proteoliposomes contained ~10–20 molecules of Tom40 per liposome. Circular dichroism spectra were recorded using a Jasco-J-600A spectropolarimeter as described[13]. Samples were adjusted to the same protein concentration ($100 \pm 30\ \mu g$) and spectra were averaged ($n = 30$) to improve the signal:noise ratio. For digestion with trypsin, proteoliposomes were concentrated by discontinuous sucrose or Ficoll density gradient centrifugation and treated with 1–5 $\mu g\ ml^{-1}$ trypsin. Mitochondria were treated with 10–50 $\mu g\ ml^{-1}$ trypsin (the presence of other Tom proteins requires a higher concentration of trypsin in order to obtain access to Tom40 (refs 16, 17)). The preprotein Su9–DHFR and DHFR were synthesized in rabbit reticulocyte lysate in the presence of [^{35}S]methionine/cysteine[16] and incubated with Tom40-containing liposomes and Tom40-free liposomes in buffer containing 20 mM KCl and 2% (w/v) BSA, followed by addition of further KCl (concentration as in wash buffer). The liposomes were isolated by centrifugation and washed in KCl (100–200 mM)-containing buffer.

Electrophysiological measurements. Planar lipid bilayers were produced using the painting technique[13]. The resulting bilayers had a typical capacitance of $\sim 0.5\ \mu F\ cm^{-2}$ and a resistance of $>100\ G\Omega$ (root mean square $\approx$ 1 pA at 5 kHz bandwidth). After a stable bilayer was formed in symmetrical solutions of 20 mM KCl, 10 mM MOPS/Tris pH 7.0, the solution of the *cis* chamber was changed to asymmetrical concentrations (*cis* chamber: 250 mM KCl, 10 mM $CaCl_2$, 10 mM MOPS/Tris pH 7.0) by adding concentrated solutions of KCl and $CaCl_2$. The liposomes were added to the *cis* compartment directly below the bilayer through the tip of a micropipette to allow the flow of the liposomes across the bilayer. If necessary, the solution in the *cis* chamber was stirred to promote fusion. After fusion, the electrolytes in both compartments were changed to the final composition by perfusion. The Ag/AgCl electrodes were connected to the chambers through 2 M KCl–agar bridges. The electrode of the *trans* compartment was directly connected to the headstage of a current amplifier (EPC 7, List Medical). Reported membrane potentials are referred to the *trans* compartment. The amplified currents were recorded on a modified DAT recorder digitized at sampling intervals of 0.05–0.2 ms.

Received 8 June; accepted 7 July 1998.

1. Schatz, G. & Dobberstein, B. Common principles of protein translocation across membranes. *Science* **271,** 1519–1526 (1996).
2. Neupert, W. Protein import into mitochondria. *Annu. Rev. Biochem.* **66,** 863–917 (1997).
3. Pfanner, N., Craig, E. A. & Hönlinger, A. Mitochondrial preprotein translocase. *Annu. Rev. Cell Dev. Biol.* **13,** 25–51 (1997).
4. Moran, O., Sandri, G., Panfili, E., Stühmer, W. & Sorgato, C. Electrophysiological characterization of contact sites in brain mitochondria. *J. Biol. Chem.* **265,** 908–913 (1990).
5. Lohret, T. A., Jensen, R. E. & Kinnally, K. W. Tim23, a protein import component of the mitochondrial inner membrane, is required for normal activity of the multiple conductance channel, MCC. *J. Cell Biol.* **137,** 377–386 (1997).
6. Juin, P., Thieffry, M., Henry, J.-P. & Vallette, F. M. Relationship between the peptide-sensitive channel and the mitochondrial outer membrane protein translocation machinery. *J. Biol. Chem.* **272,** 6044–6050 (1997).
7. Dihanich, M., Schmidt, A., Oppliger, W. & Benz, R. Identification of a new pore in the mitochondrial outer membrane of a porin-deficient yeast mutant. *Eur. J. Biochem.* **181,** 703–708 (1989).
8. Baker, K. P., Schaniel, A., Vestweber, D. & Schatz, G. A yeast mitochondrial outer membrane protein essential for protein import and cell viability. *Nature* **348,** 605–609 (1990).
9. Mannella, C. A., Neuwald, A. F. & Lawrence, C. E. Detection of likely transmembrane β-strand regions in sequences of mitochondrial pore proteins using the Gibbs sampler. *J. Bioenerg. Biomembr.* **28,** 163–169 (1996).
10. Schmid, B., Krömer, M. & Schulz, G. E. Expression of porin from *Rhodopseudomonas blastica* in *Escherichia coli* inclusion bodies and folding into exact native structure. *FEBS Lett.* **381,** 111–114 (1996).
11. Sreerama, N. & Woody, R. W. Protein secondary structure from circular dichroism spectroscopy: combining variable selection principle and cluster analysis with neural network, ridge regression and self-consistent methods. *J. Mol. Biol.* **242,** 497–507 (1994).
12. Hille, B. in *Ionic Channels of Excitable Membranes*. Ch. 9, 11 (Sinauer, Sunderland, Massachusetts, 1992).
13. Hinnah, S., Hill, K., Wagner, R., Schlicher, T. & Soll, J. Reconstitution of a chloroplast protein import channel. *EMBO J.* **16,** 7351–7360 (1997).
14. Smart, O. S., Breed, J., Smith, G. R. & Sansom, M. S. A novel method for structure-based prediction of ion channel conductance properties. *Biophys. J.* **72,** 1109–1126 (1997).
15. Krasilnikov, O. V., Sabirov, R. Z., Ternovsky, V. L., Merzliak, P. G. & Muratkhodjaev, J. N. A simple method for the determination of the pore radius of ion channels in planar lipid bilayer membranes. *FEMS Microbiol. Immunol.* **5,** 93–100 (1992).
16. Alconada, A., Gärtner, F., Hönlinger, A., Kübrich, M. & Pfanner, N. Mitochondrial receptor complex from *Neurospora crassa* and *Saccharomyces cerevisiae*. *Methods Enzymol.* **260,** 263–286 (1995).
17. Dietmeier, K. *et al*. Tom5 functionally links mitochondrial preprotein receptors to the general import pore. *Nature* **388,** 195–200 (1997).
18. Dekker, P. J. T. *et al*. The Tim core complex defines the number of mitochondrial translocation contact sites and can hold arrested preproteins in the absence of matrix Hsp70-Tim44. *EMBO J.* **16,** 5408–5419 (1997).
19. Allison, D. S. & Schatz, G. Artificial mitochondrial presequences. *Proc. Natl Acad. Sci. USA* **83,** 9011–9015 (1986).
20. Brix, J., Dietmeier, K. & Pfanner, N. Differential recognition of preproteins by the purified cytosolic domains of the mitochondrial import receptors Tom20, Tom22, and Tom70. *J. Biol. Chem.* **272,** 20730–20735 (1997).
21. Rapaport, D., Neupert, W. & Lill, R. Mitochondrial protein import: Tom40 plays a major role in targeting and translocation of preproteins by forming a specific binding site for the presequence. *J. Biol. Chem.* **272,** 18725–18731 (1997).
22. Mayer, A., Neupert, W. & Lill, R. Mitochondrial protein import: reversible binding of the presequence at the *trans* side of the outer membrane drives partial translocation and unfolding. *Cell* **80,** 127–137 (1995).
23. Vestweber, D. & Schatz, G. DNA-protein conjugates can enter mitochondria via the protein import pathway. *Nature* **338,** 170–172 (1989).
24. Künkele, K.-P. *et al*. The preprotein translocation channel of the outer membrane of mitochondria. *Cell* **93,** 1009–1019 (1998).
25. Matlack, K. E. S., Mothes, W. & Rapoport, T. A. Protein translocation: tunnel vision. *Cell* **92,** 381–390 (1998).
26. Vestweber, D., Brunner, J., Baker, A. & Schatz, G. A 24K outer-membrane protein is a component of the yeast mitochondrial protein import site. *Nature* **341,** 205–209 (1989).
27. Kiebler, M. *et al*. Identification of a mitochondrial receptor complex required for recognition and membrane insertion of precursor proteins. *Nature* **348,** 610–616 (1990).
28. Söllner, T. *et al*. Mapping of the protein import machinery in the mitochondrial outer membrane by crosslinking of translocation intermediates. *Nature* **355,** 84–87 (1992).
29. Hönlinger, A. *et al*. The mitochondrial receptor complex: Mom22 is essential for cell viability and directly interacts with preproteins. *Mol. Cell. Biol.* **15,** 3382–3389 (1995).
30. Bolliger, L., Junne, T., Schatz, G. & Lithgow, T. Acidic receptor domains on both sides of the outer membrane mediate translocation of precursor proteins into yeast mitochondria. *EMBO J.* **14,** 6318–6326 (1995).

Acknowledgements. We thank P. J. T. Dekker, B. Guiard, M. Kiebler, W. Kühlbrandt, D. Mills, J. Brix, S. C. Hinnah and H. Martin for materials, advice and discussion. This work was supported by the Deutsche Forschungsgemeinschaft, Sonderforschungsbereich 388, the Fonds der Chemischen Industrie (N.P.), the Sonderforschungsbereich 171 (R.W.) and a longterm fellowship of the Alexander-von-Humboldt Foundation (M.T.R.)

Correspondence and requests for materials should be addressed to N.P. (e-mail: pfanner@ruf.uni-freiburg.de).

Drosophila CBP represses the transcription factor TCF to antagonize Wingless signalling

Lucas Waltzer & Mariann Bienz

MRC Laboratory of Molecular Biology, Hills Road, Cambridge CB2 2QH, UK

T-cell factor (TCF), a high-mobility-group domain protein, is the transcription factor activated by Wnt/Wingless signalling[1–4]. When signalling occurs, TCF binds to its coactivator, beta-catenin/Armadillo, and stimulates the transcription of the target genes of Wnt/Wingless by binding to TCF-responsive enhancers[1,5]. Inappropriate activation of TCF in the colon epithe-